///VSP/// Journal of Biomaterials Science 20 (2009) 2117–2128

Journal of BIOMATERIALS SCIENCE
www.brill.nl/jbs

Biocompatibility, Alignment Degree and Mechanical Properties of an Electrospun Chitosan–P(LLA-CL) Fibrous Scaffold

Feng Chen [a,b], **Yan Su** [a], **Xiumei Mo** [a,*], **Chuanglong He** [a], **Hongsheng Wang** [a] **and Yoshito Ikada** [c]

[a] College of Chemistry, Chemical Engineering and Biotechnology, Donghua University, 2999 North Renmin Road, Songjiang District, Shanghai 201620, P. R. China

[b] State Key Laboratory of High Performance Ceramics and Superfine Microstructure, Shanghai Institute of Ceramics, Chinese Academy of Sciences, Shanghai 200050, P. R. China

[c] Department of Indoor Environmental Medicine, Nara Medical University, Nara, Japan

Received 17 August 2008; accepted 18 December 2008

Abstract

Chitosan–poly(L-lactide-co-ε-caprolactone) (P(LLA-CL)) complex fibers, fibrous mats and a tubular scaffold have been obtained through electrospinning. Due to their high porosity, there were more porcine iliac artery endothelial cells (PIECs) attached to fiber mats than to tissue-culture plate (TCP) and coverslips. The cells could grow and spread well on nanofiber mats. There were many of native extracellular matrix (ECM)-like colloids above and under the surface of fibrous mats after cell culturing. The two-dimensional fast Fourier transform (2-D FFT) approach was used to analysis alignment degree of fibers collected on a rotary mandrel. The relations among mechanical properties, alignment degree, fiber diameter and rotary speed are discussed. Aligned fibers with various alignment degrees could be found through adjusting rotary speed. Fiber alignment was the variable most closely associated with the regulation of stress and strain. In this study, we show a feasible approach for producing scaffold with controllable mechanical property for soft tissue engineering through electrospinning.

Keywords

Electrospinning, chitosan, poly(L-lactic acid-co-ε-caprolactone), mechanical properties, tissue engineering

1. Introduction

Native extracellular matrix (ECM) is a chemically and physically cross-linked complex network of three important classes of biomacromolecules secreted locally

[*] To whom correspondence should be addressed. Tel.: (86-21) 6779-2653; Fax: (86-21) 6779-2653; e-mail: xmm@dhu.edu.cn

 DOI:10.1163/156856208X400492

by cells. In a typical connective tissue, structural fibers such as collagen fibers and elastin fibers, ECM diameters range from several tens to several hundreds of nanometers. The nanoscale fibers entangle with each other to form a non-woven mesh that provides tensile strength and elasticity for the tissues [1]. Major load-bearing collagenous soft tissues exhibit an exponential-like stress–strain response, largely due to how the constituent collagen fibers gradually straighten as the tissue bears increasing load levels, as well as the subtle contributions of elastin [2, 3]. Since mechanical loads can vary spatially and temporally within the tissues of an organ, they exhibit complex, mechanically anisotropic behaviors optimized for their respective physiological function [2]. While an ultimate goal of tissue engineering is the precise duplication of native tissue function, thus, it is necessary to establish an approach for producing functional replacements with controllable mechanical property.

Electrospinning has been recognized as an efficient technique for fabricating polymer nanofibers which could mimic the native fiber structure of ECM and be widely used in the biomedical area [4–6]. Electrospinning involves applying a high voltage to the polymer solution. The free end of the solution jet will follow a chaotic path as it travels toward the grounded collection plate [7, 8]. Therefore, it is difficult to control the spinning process and the fabric structure. It is well known that materials with ordered microstructures may possess specific functions useful in biomedical applications. Thus, many studies have focused on obtaining a ordered structure such as aligned fibers and patterning fabrics [9–11]. However, without an objective measurement of fabric structure, it is difficult, at best, to determine how specific degrees of anisotropy might contribute to the biological and mechanical performance of a given electrospun nanofiber scaffold. Ayres *et al.* [12–14] describe an easy method for measuring fiber alignment in electrospun scaffolds with 2-D fast Fourier transform.

Poly(L-lactide-co-ε-caprolactone) (P(LLA-CL)) has been investigated as biomaterial for surgery and drug-delivery system due to its good biocompatibility and biodegradability [15]. Chitosan is biologically renewable, biodegradable, nonantigenic and biocompatible, and has been used in wound healing [16], drug-delivery carrier [17] and tissue-engineering applications [18–20]. In our previous study, chitosan–P(LLA-CL) has been used to fabricate nanofibers, and the process of electrospinning, prosity and mechanical properties of fabric were investigated [21]. In this study, fibrous tubular scaffold was obtained, and aligned fibers and their mechanical properties, as well as the biocompatibility of nanofibrous mats have been studied and discussed.

2. Materials and Methods

2.1. Materials

A co-polymer of P(LLA-CL) (50:50), which has a composition of 50 mol% L-lactide, was used. Squid pen chitosan with a deacetylation degree of 60% was purchased from Fine Chemical Sales Carbohydrate Chemistry Team Industrial Research (New Zealand). Trifluoroacetic acid (TFA) was purchased from Shanghai Runjie Chemical Reagent (China). 1,1,1,3,3,3-Hexafluoro-2-propanol (HFIP) was purchased from Daikin Industries (Japan). Porcine iliac artery endothelial cells (PIECs) were obtained from the Institute of Biochemistry and Cell Biology (Chinese Academy of Sciences, China). Unless noted, all culture media and reagents were purchased from Gibco Life Technologies (USA).

2.2. *Electrospinning of Fibers*

Chitosan was dissolved with HFIP and TFA (9:1, v/v) at a concentration of 8 wt%, while P(LLA-CL) was dissolved with HFIP at a concentration of 8 wt%. When both of them have been dissolved completely, the solutions were mixed and stirred for 30 min at room temperature. The solution for electrospinning was fed into a plastic syringe with a needle (inner diameter 0.21 mm). A syringe pump (789100C, Cole-Palmer, USA) was used to feed the solution to the needle with a feed rate of 1.5 ml/h. Electrospinning voltage was applied to the needle at 15 kV using a high-voltage power supplier (BGG6-358, BMEI, China). A grounded foil can be used to collected fibers at fixed distance (18 mm from the needle tip). As to fabricate small-diameter tubular scaffold, a grounded mandrel ($D = 4$ mm) was chosen instead of foil to collect fibers and fabricate porous tubular scaffold. The length and thickness of tubular scaffold can be determined by the length of mandrel and electrospinning time.

2.3. *Study of PIECs on Fiber Mats*

PIECs were cultured in 1640 medium with 10% fetal serum, 100 U/ml penicillin and 100 U/ml streptomycin in a humidified incubator (BB-15, Heraeus, Germany) with 5% CO_2 at 37°C, and the medium was replaced every 3 days. The solutions with different content of chitosan in blend (0, 20, 40, 60 and 80 wt%) were electrospun into fibers. The coverslips (14 mm in diameter) were put onto the aluminum foil to collect the electrospun fiber mats fabricated from above mixed solutions. In 1 h, thin mats could be found on the coverslips. Then the mats were fixed in 24-well plates with stainless ring and sterilized with 75% alcohol solution, which was replaced with phosphate-buffered saline solution (PBS) after 2 h for washing. These mats were used for viability test with PIECs. For the cell attachment and proliferation test, PIECs were seeded onto the fiber mats, coverslips and TCP at a density of 3.0×10^4 cells/cm^2. At 2, 4 and 12 h after cell seeding, unattached cells were washed out and attached cells were quantified by MTT assay (Sigma, USA) and Enzyme-labeled Instrument (MK3, Thermo, USA). Data are representative of three independent experiments and all data points are plotted as means ± standard deviation (SD) ($n = 3$).

For the morphology study of PIECs cultured on the mats, the samples were washed with PBS and then fixed with 4% glutaraldehyde for 45 min at 4°C after 24 h culture. For investigation of fiber mats surface after cells culturing, the samples were trypsinized for 20 min on day 7 after cell seeding and washed with PBS. Thereafter, the samples were dehydrated in 50, 75, 90 and 100% alcohol and dried under vacuum. The samples were sputter coated with gold and observed with SEM at a voltage of 15 kV.

2.4. Measuring Fiber Alignment

To investigate the relationship between mechanical properties and rotary speed, a mandrel ($D = 2$ cm; Fig. 1), rotating at high speed varying from 500 to 4000 rpm, was used to produce fibers with controllable orientation. After 30–60 min, electrospun fiber mats were taken off from the mandrel, sputter coated with gold and observed with SEM at a voltage of 15 kV. Measuring of fiber alignment was achieved using 2-D fast Fourier transform (2-D FFT) [12]. Grayscale 8-bit images were cropped to 2048 × 2048 pixels for analysis. Image J software (NIH, USA) supported by an oval profile plug-in was used to conduct 2-D FFT analysis. Pixel intensities were summed along a radius from the center to the edge of the image to quantify the relative contribution of objects oriented in that direction. All alignment data were normalized to a baseline value of 0 and plotted in arbitrary units from 0 to approx. 0.25.

2.5. Mechanical Measurements

Mechanical measurements were done by applying tensile test loads to specimens. In this study, specimens were prepared according to the method described by Huang *et al.* [22]. First, a white paper was cut into templates with width × gauge length = 10 mm × 50 mm, and double-sided tapes were glued onto the top and bottom areas of one side. Secondly, the specimens were carefully peeled off from collector and single side tapes were applied onto the gripping areas as end-tabs. The resulting

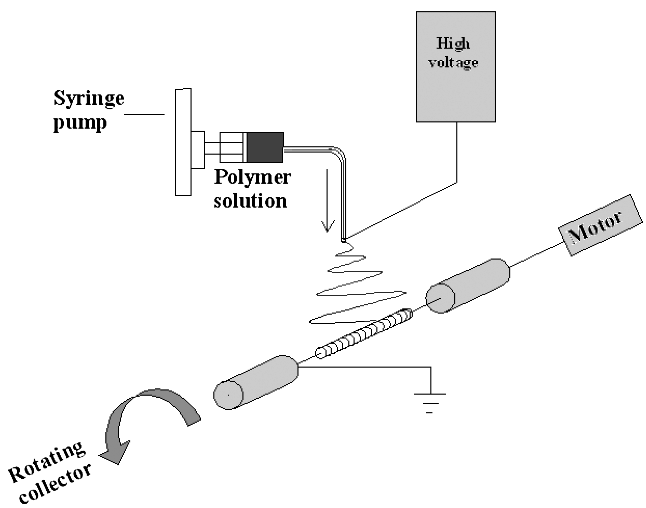

Figure 1. Schematic illustration of collecting electrospun fibers on a rotating mandrel.

specimens had a planar dimension of width $\times$ gauge length $=$ 10 mm $\times$ 30 mm. Mechanical properties were tested by a materials testing machine (H5K-S, Hounsfield, UK) at 20°C, a relative humidity of 65% and elongation speed of 10 mm/min. Data are representative of three independent experiments and all data points are plotted as means $\pm$ SD ($n = 3$).

2.6. Statistical Analysis

Statistical analysis was performed using Origin 7.5 (OriginLab, USA). Samples that passed normality and equal variance tests were evaluated using a one-way analysis of variance (ANOVA). The priori alpha value was set at 0.05 with significance defined as $P \leqslant 0.05$.

3. Results and Discussion

3.1. Microstructure of Fibers Mats and Tubular Scaffold

Chitosan–P(LLA-CL) blended solution was easy to be electrospun into fibers and fabric. Figure 2 shows a photograph and SEM image of electrospun membrane from solution with blend ratio of 2:8 (chitosan/P(LLA-CL)) at a concentration of 8 wt%. The fibers collected as a non-woven mat on the target collector, and the fabric constructed with these fibers was flexile. The broken stress and strain of these blended fibrous membranes were as high as to 3.6 ± 0.63 MPa and 102.5 ± 17.33%, respectively. Otherwise, both of them could increase with increasing P(LLA-CL) content [21]. The mechanical properties could be adjusted to the requirement through changing the blend ratio of chitosan to P(LLA-CL).

After drying under vacuum, the scaffold was carefully pulled off from mandrel. As Fig. 3 shows, the tubular scaffold showed good morphology. Compared with the primary scaffold, no visible structural distortion could be found after extending the cross-section of the scaffold with a medical forceps. From SEM images of the cross-section, it was easy to find that the electrospun blend fibers could maintain

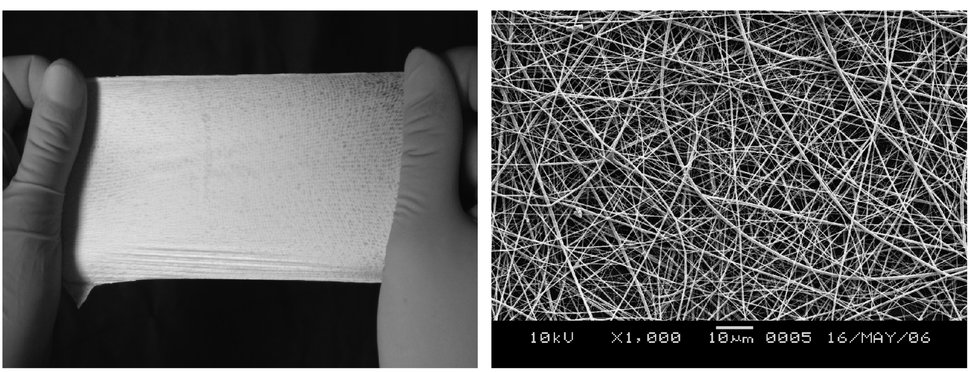

Figure 2. A photograph and an SEM micrograph of a electrospun fiber mat containing 80% P(LLA-CL).

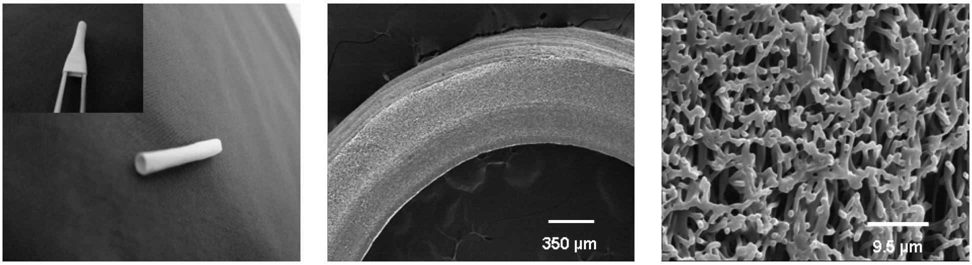

(a) (b) (c)

Figure 3. Electrospun fibrous tubular scaffold with chitosan–P(LLA-CL) blended solution. (A) The morphology of the tubular scaffold, (B) the SEM images of the cross-section, (C) magnified morphology of the cross-section microstructure.

their structure in the scaffold. As a magnified image (Fig. 3C) shows, the tubular scaffold presents a high porosity.

Electrospun fibrous tubular scaffolds behaved like an elastomer due to the presence of a large portion of P(LLA-CL 50:50), which was a co-polymer of L-lactide and caprolactone. In a previous report, P(LLA-CL 50:50) was flexible and elastic with relatively good mechanical properties, strain recoveries of more than 95% at 100% strain [23]. The high porosity of tubular scaffold could be explained by presence of chitosan in the blend. The content of chitosan could increase the conductivity of solution. The fiber diameter varied with the blend ratio. The average diameter decreased from 124 to 426 nm with decreasing blend ratio of chitosan to P(LLA-CL) from 8:2 to 0:10. Otherwise, more electronic charges would be carried by the electrospinning jet, causing the stronger repulsive forces among fibers during deposition onto the collector [21].

3.2. *Study of PIECs on Fiber Mats*

The attachment of PIECs to chitosan–P(LLA-CL) fibers mats, TCPs and coverslips is shown in Fig. 4. PIECs showed good attachment to the electrospun chitosan–P(LLA-CL) composite mats. Significantly, the number of PIECs attached to fiber mats in 12 h was higher than to TCP and coverslips ($P < 0.05$). However, there were no significant differences among the electrospun fibrous mats with different blend ratios. As shown in Fig. 5A–D, the fiber mats showed high porosity, and the cells could grow and spread well on fiber mats with different blend ratios of chitosan after 24 h culture. From Fig. 5C and 5D, we noticed that a small number of cells could migrate into the mats and grow under the fibers. Figure 5E shows the morphology of cells on fibers mat contained 40% chitosan after 7 days culture. In order to investigate the surfaces of fibrous mats under the cell layer after long-term cell culturw, the cells were trypsinized off the surface of the mats, and then the mats were observed under SEM. Compared with new fabricated fibers the surface of cell-treated fibers was rougher, and there are many native ECM-like colloids above and under the surface of the mat (Fig. 5E, arrow).

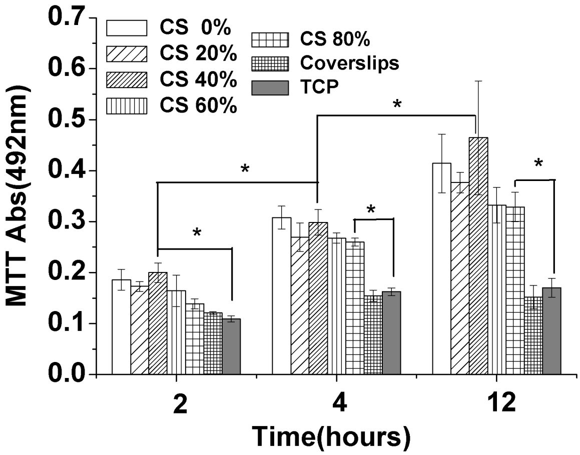

Figure 4. Attachment of PIECs on chitosan–P(LLA-CL) nanofibers mats, $^*P < 0.05$.

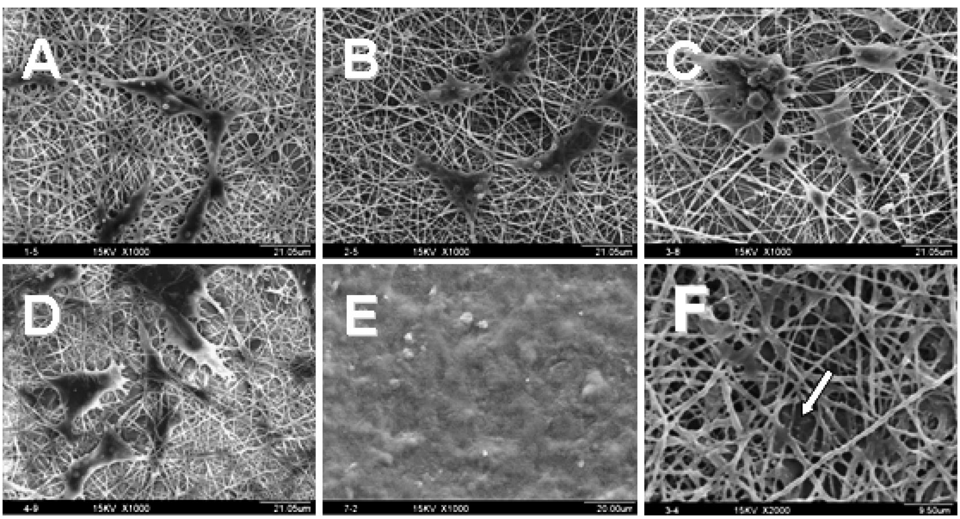

Figure 5. Morphology of PIECs after 24 h culture on nanofiber mats containing different amounts of chitosan (A) 0%, (B) 20%, (C) 40%, (D) 60%. Panel (E) shows cell morphology on fibrous mat containing 40% chitosan after 7 days culturing, (F) shows the surface morphology of fibrous mats (40% chitosan) which were trypsinized after one week culturing of PIECs. The white arrow shows ECM-like colloid.

Compared with the smooth surface of TCP and coverslips, electrospun fiber mats with high porosity and rough surface could facilitate cell adhesion. The porosity of blended fibrous membranes varied from $64.5 \pm 1.5\%$ to $86.5 \pm 1.5\%$, and increased with the increasing weight ratio of chitosan to P(LLA-CL) [21]. However, the results of MTT assays did not show an increase with increasing chitosan content in fibers. This may be because the increase of chitosan content in complex fibers could lead to more chitosan dissolved in the cell-culture medium. Electrospun chitosan fibers without cross-linking could not maintain their structure in aqueous solution. The result of this process may affect the structure of fibrous mats and the attachment of cells onto the mats. The cells which could grow and spread well on nanofibrous mats after 24 h culture may suggest that the surface of blended fiber is suitable for cell attachment and migration. The reason may be that chitosan has structural characteristics similar to glycosaminoglycans and has distinctive biological properties, including good biocompatibility. It has been reported that chitosan is able to promote cell attachment and maintain characteristic morphology and viability of various cells such as human osteoblasts and chondrocytes [24].

3.3. Alignment Degree and Mechanical Properties

It is not easy to measure stress, strain and fiber alignment, and difficult to describe relationships among these parameters in a small-diameter tubular fibrous scaffold for tissue engineering. In this work, a large diameter mandrel was used to instead of small ones to collect fibers at different rotary speeds. Then the membranes constructed with these fibers would be measured for alignment degree and mechanical properties. From SEM images of chitosan–P(LLA-CL) blend electrospun onto a rotating mandrel (Fig. 6), the filaments are deposited along the axis of rotation. The target mandrel rotating at 500–4000 rpm results in a trend of fibers depositing into a linear alignment. Under the conditions of this experiment, the linear speed of the surface was approximately 0.523–4.187 m/s. However, due to the limited diameter of rotary mandrel, the linear speed was not high enough to meet the requirement of complete parallel fibers, even with an angular velocity of 4000 rpm.

Figure 6D–F shows raw output of the 2-D FFT alignment analysis of aligned fibers. Pixel intensities and the distribution of the intensities of this output image correlate to the directional content of the original image. The slender profiles of the silhouette in raw output of the 2-D FFT indicate the occurrence of fiber alignment. Figure 6G–I shows radial plots of the summations of relative pixel intensity at a radius *versus* the angle (°) caused by the inherent symmetry of the raw 2-D FFT output. From the results, we can see that the peaks increase with the rotary speed. A sharper, narrower peak at 90 and 270° indicates the general direction in which the fiber population is oriented. Figure 6J–L shows the typical tensile stress–strain curves of blended fibers mats deposited on rotary mandrel. Both the tensile strength and the ultimate strain increased with the increasing rotary speed.

Figure 7A and 7B shows the relationship between mechanical properties in dry and wet condition and rotary speed, respectively. As the histograms show, the stress and strain exhibited and incremental trend, both in dry and wet conditions. Otherwise, the diameter of fibers increased with increasing rotary speed of collector (Fig. 7C), possibly because of the decreasing fiber deposition time. The rotary mandrel could lead the changing of pathway of fibers through pulling the fibers for deposition. The process may result in decreasing volatilization time of solvent, and affect the diameter of fibers. The relation of mechanical properties with the changing of alignment and diameters is illustrated in Fig. 8. As the FFT alignment degree

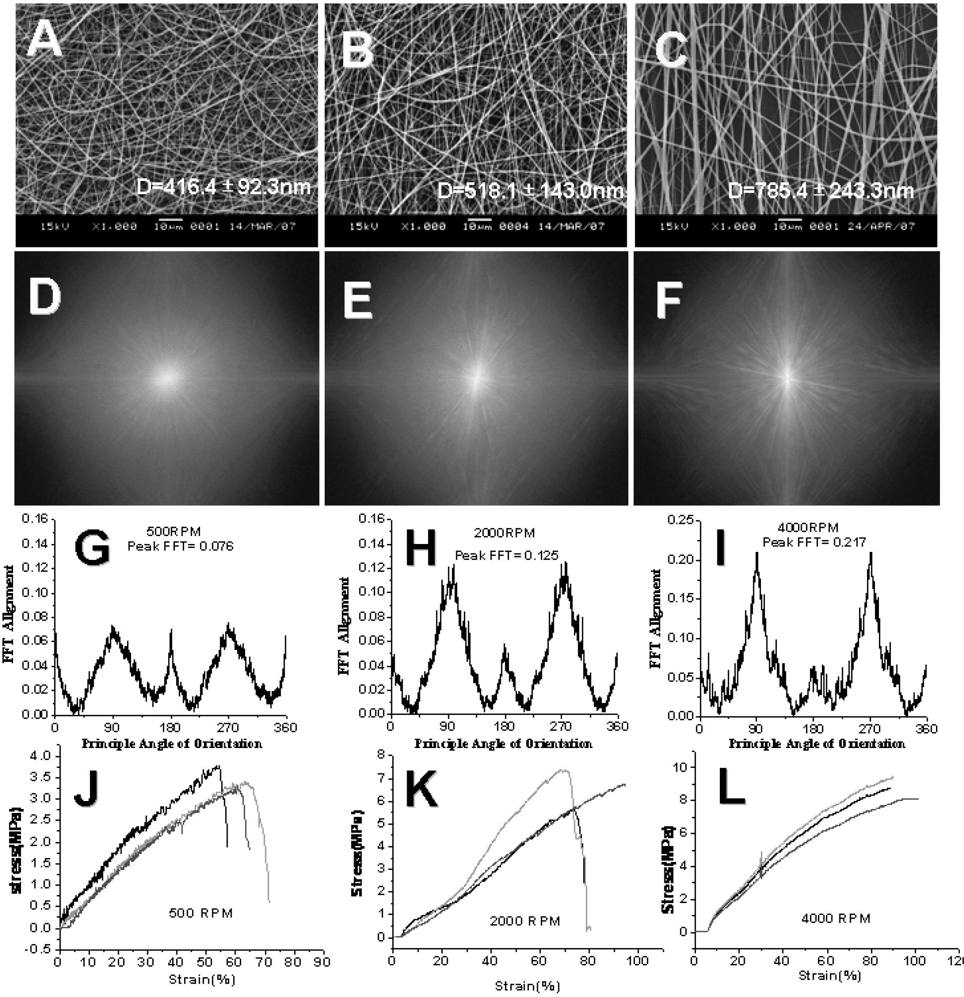

Figure 6. Investigation of morphology, alignment degree and mechanical properties of electrospun fibers collected by a rotating mandrel with different rotary speed, (A) 500 rpm, (B) 2000 rpm, (C) 4000 rpm. (D–F) Raw output of the 2-D FFT alignment analysis of electrospun fibers corresponding to (A–C). (G–I) Radial plot of the summations of relative pixel intensity at a radius *versus* the angle (°) caused by the inherent symmetry of the raw 2-D FFT output. (J–L) Stress–strain curves of electrospun fibers with controllable alignment in dry condition.

increased from 0.076 to 0.217 and the diameter from 416 to 785 nm, the curves of both stress and strain exhibited incremental changes, and the trend of the curves was different in dry and wet conditions. There were obvious relative increments of stress and strain of fibers with increasing alignment degree and diameter.

The stress- and strain-at-break of fiber membranes have been improved by increasing the rotary speed. The increasing diameter might affect the mechanical properties of fabric through changes of the properties of a single fiber. The bigger

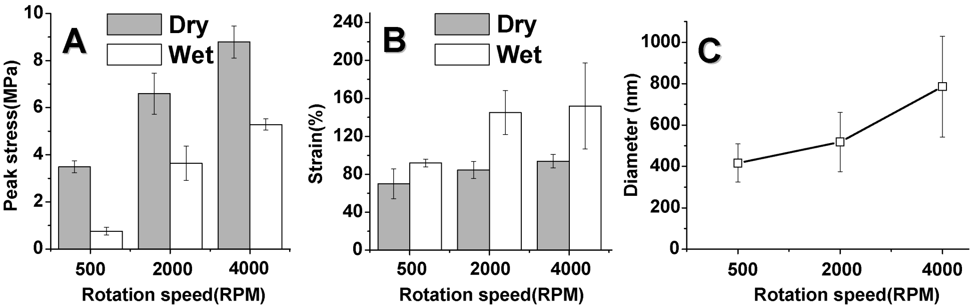

Figure 7. Relations of mechanical properties and diameters with rotary speed. (A, B) Peak stress and strain of electrospun fabrics collected by a rotating mandrel at different rotary speed. (C) Change of diameters with increased rotary speed, $^*P < 0.05$.

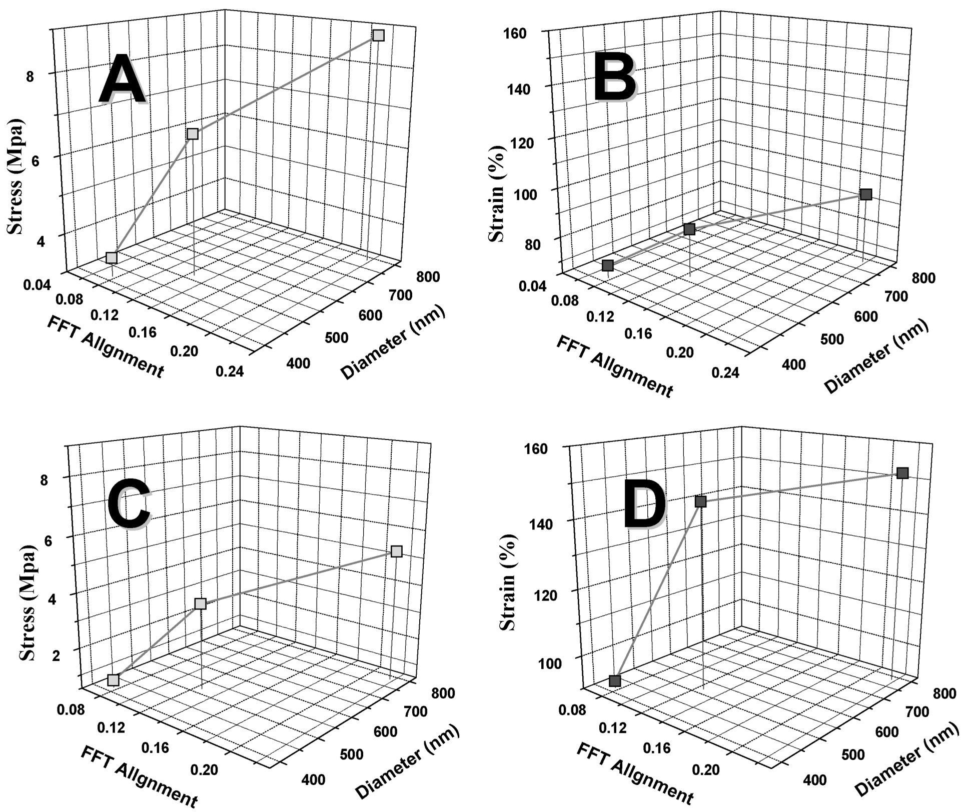

Figure 8. The relations of mechanical properties with fiber alignment degree and diameters in dry (A, B) and wet (C, D) conditions.

dimension of fibers might lead to higher stress- and strain-at-break. The alignment degree is also important for mechanical properties through changing array of fibers in the fabric. As shown in Figs 2 and 6A, the fibers which were collected by plate and rotation collector with low speed show no alignment; alignment could be obtained by increasing the rotation speed (Fig. 6B and 6C). The alignment of fibers was promoted by increasing the rotation speed of the mandrel. The higher alignment of fibers along the direction of tensile loading leads to more fibers that support the tensile force in the equal mat section. At the same time, it is also in favor of slipping between two fibers in the mat. Fiber alignment was the variable most closely associated with the regulation of peak stress, peak strain. Incremental changes, as judged by the FFT method, in the proportion of fibers that were aligned along a specific axis induced incremental changes in peak stress in the fibers scaffolds. Both broken stress and strain have been improved by adjusting the rotation speed of the mandrel collector. Finally, it was possible to establish an approach to produce a functional scaffold with controllable mechanical properties for soft-tissue engineering by electrospinning.

4. Conclusion

A chitosan–P(LLA-CL) blended solution was easy to be electrospun into fibers, and to form fiber mats and nanofibrous tubular scaffolds. Due to the high porosity, there were more PIECs attached to fiber mats than to TCP and coverslips. The cells could grow and spread well on fiber mats. Compared with new fabricated fibers, the surface of cell-treated fibers were rougher, and there were many ECM-like colloids above and under the surface of the mat.

The nanofibrous tubular scaffold showed good morphology. 2-D FFT was used to analyze the alignment degree of fibers collected on a rotary mandrel. The relation of mechanical properties, alignment degree, fiber diameter and rotary speed was discussed. Aligned fibers with various alignment degrees could be fabricated by adjusting the rotary speed. Fibers alignment was the variable most closely associated with the regulation of stress and strain. In this study, it performed a feasible approach for producing a scaffold with controllable mechanical properties for soft-tissue engineering by electrospinning.

Acknowledgements

This research was supported by the National Nature Science Foundation of China (30570503), Shanghai Sci. & Tech. Committee China (05DJ14006, 05PJ14013), Natural Science Foundation of Shanghai (07ZR14001) and the 111 project (B07024).

References

1. Z. W. Ma, M. Kotaki, R. Inai and S. Ramakrishna, *Tissue Eng.* **11**, 101 (2005).
2. Y. C. Fung, *Biomechanics: Mechanical Properties of Living Tissues*, 2nd edn. Springer, Berlin (1993).
3. Y. Lanir, *J. Biomech.* **16**, 1 (1983).

4. S. Liao, B. Li, Z. W. Ma, H. Wei, C. Chan and S. Ramakrishna, *Biomed. Mater.* **1**, 45 (2006).
5. H. Yoshimoto, Y. M. Shin, H. Terai and J. P. Vacanti, *Biomaterials* **24**, 2077 (2003).
6. C. Y. Xu, R. Inai, M. Kotaki and S. Ramakrishna, *Tissue Eng.* **10**, 1160 (2004).
7. D. H. Reneker, A. L. Yarin, H. Fong and S. Koombhongse, *J. Appl. Phys.* **87**, 4531 (2000).
8. Y. M. Shin, M. M. Hohman, M. P. Brenner and G. C. Rutledge, *Polymer* **42**, 9955 (2001).
9. J. A. Matthews, G. E. Wnek, D. G. Simpson and G. L. Bowlin, *Biomacromolecules* **3**, 232 (2002).
10. W. E. Teo, M. Kotaki, X. M. Mo and S. Ramakrishna, *Nanotechnology* **16**, 918 (2005).
11. D. M. Zhang and J. Chang, *Adv. Mater.* **19**, 3664 (2007).
12. C. E. Ayres, S. Jha, H. Meredith, J. R. Bowman, G. L. Bowlin, S. C. Henderson and D. G. Simpson, *J. Biomater. Sci. Polymer Edn* **19**, 603 (2008).
13. C. E. Ayres, G. L. Bowlin, S. C. Henderson, L. T. Taylor, J. Shultz, J. Alexander, T. A. Telemeco and D. G. Simpson, *Biomaterials* **27**, 5524 (2006).
14. C. E. Ayres, G. L. Bowlin, R. Pizinger, L. T. Taylor, C. A. Keen and D. G. Simpson, *Acta Biomater.* **3**, 651 (2007).
15. Y. Ikada, *Tissue Engineering: Fundamentals and Applications*. Academic Press, San Diego, CA (2006).
16. K. Aiedeh, E. Gianasi, I. Orienti and V. Zecchi, *J. Microencapsul.* **14**, 567 (1997).
17. J. Berger, M. Reist, J. M. Mayer, O. Felt and R. Gurny, *Eur. J. Pharm. Biopharm.* **57**, 19 (2004).
18. Y. Zhang and M. Q. Zhang, *J. Biomed. Mater. Res. A* **55**, 304 (2001).
19. K. Yagi, N. Michibayashi, N. Kurikawa, Y. Nakashima, T. Mizoguchi, A. Harada, S. Higashiyama, H. Muranaka and M. Kawase, *Biol. Pharm. Bull.* **20**, 1290 (1997).
20. P. R. Klokkevold, L. Vandemark, E. B. Kenney and G. W. Bernard, *J. Periodontol.* **67**, 1170 (1996).
21. F. Chen, X. Q. Li, X. M. Mo, C. L. He, H. S. Wang and Y. Ikada, *J. Biomater. Sci. Polymer Edn* **19**, 677 (2008).
22. Z. M. Hang, Y. Z. Zhang, S. Ramakrishna and C. T. Lim, *Polymer* **45**, 5361 (2004).
23. O. Jean, S. H. Lee, S. H. Kim, Y. M. Lee and Y. H. Kim, *Macromolecules* **36**, 5585 (2003).
24. N. Bhattarai, D. Edmondson, O. Veiseh, F. A. Matsen and M. Zhang, *Biomaterials* **26**, 6176 (2005).